Journal of Cellular Biochemistry 102:183–195 (2007)

Enhancement of Neovascularization with Mobilized Blood Cell Transplantation: Supply of Angioblasts and Angiogenic cytokines

Bin Zhou,[1] Peng Xia Liu,[1] Hai Feng Lan,[1] Zhi Hong Fang,[1] Zhi Bo Han,[1,2] He Ren,[1] Man-Chiu Poon,[1,3] and Zhong Chao Han[1,2]*

[1]State Key Laboratory of Experimental Hematology, National Research Center for Stem Cell Engineering and Technology, Institute of Hematology, Chinese Academy of Medical Sciences and Peking Union Medical College, Tianjin, China
[2]National Engineering Research Center of Cell Products, AmCellGene Co. Ltd, TEDA, Tianjin, China
[3]Departments of Medicine, University of Calgary, Alberta, Canada

Abstract We have recently provided evidence that transplantation of G-CSF mobilized peripheral blood mononuclear cells (M-PBMNCs) improves limb ischemia in diabetic patients. This method represents a simple, safe, effective, and novel therapeutic approach for diabetic ischemia. Here we investigated the mechanisms by which mobilized blood cells transplantation improves limb ischemia. Unilateral hindlimb ischemia was surgically induced in streptozotocin-induced diabetic nude mice, and they were intramuscularly injected 10^6 M-PBMNCs, or human umbilical vein endothelial cells (HUVECs), PBS controls. We compared their blood-flow restoration via laser Doppler perfusion image (LDPI), angiogenesis via histological determination of capillary density. Physiological and histological assessment revealed an acceleration of ischemia recovery and increase in capillary density with less apoptosis in M-PBMNCs group, compared with those in HUVECs and PBS groups. In vivo noninvasive imaging and immunofluorescence revealed the survival, migration, proliferation, differentiation, and incorporation of M-PBMNCs into foci of vessel networks. More angioblasts were from blood cells after mobilization, and they also produced a number of antiapoptotic and proagniogenic factors that promoted angiogenesis in vivo. M-PBMNCs and its conditioned medium augmented the vessel formation in matrigel plugs in vivo. Thus, transplantation of M-PBMNCs achieved therapeutic neovascularization via supply of abundant angioblasts and angiogenic factors. J. Cell. Biochem. 102: 183–195, 2007.

Key words: neovascularization; angioblasts; angiogenic factors; M-PBMNCs

Diabetic foot syndrome, one of the severe complications in the late stage of diabetes, is now a major health problem, since the amputation rate is as high as 28,000 per year in the US [Eckardt et al., 2003]. With time, endothelial cell loss by apoptosis as well as arteriole and capillary occlusion lead to microvascular rarefaction, which favors the formation of nonhealing limb ulcers and limits the benefit of revascularization [Currie et al., 1998; Emanueli et al., 2002]. To induce angiogenesis, investigators have delivered VEGF, bFGF, etc. [Folkman, 1998; Rajagopalan et al., 2001; Simons et al., 2002]. Implantation of mononuclear cells that are rich in angiogenic factors and cytokines [Iba et al., 2002] may provide a cocktail of angiogenic factors to provoke a reparative process. Thus, combination of various angiogenic factors or cell-based therapy may be preferable in future therapies [Hasson et al., 2005].

At present, a great deal of interest has arisen in the potential of cell-based strategies in repairing of ischemic damage. Hematopoietic progenitor cells (HSCs) that express CD34 have been shown to behave as EPCs or angioblasts

Bin Zhou and Peng Xia Liu contributed equally to this work.

Grant sponsor: Ministry of Science & Technology of China; Grant number: 863 (2003AA205060), 973 (001CB5101).

*Correspondence to: Zhong Chao Han, Institute of Hematology, Chinese Academy of Medical Sciences & Peking Union Medical College, 288 Nanjing Road, Tianjin 300020, China. E-mail: tihzchan@public.tpt.tj.cn or bzhoupmc@gmail.com

Received 28 August 2006; Accepted 9 January 2007

DOI 10.1002/jcb.21290

[Ingram et al., 2004], which when mobilized from the bone marrow could participate in postnatal neovascularization [Asahara et al., 1997] by incorporate into the endothelium of newly forming blood vessels in pathological and nonpathological conditions [Takahashi et al., 1999; Asahara et al., 1999a]. In diabetic mice, the injection of exogenous $CD34^+$ cells can accelerate the rate of restoration of flow to ischemic limbs [Schatteman et al., 2000]. Recently EPCs have now become clinically relevant, and trials of therapeutic angiogenesis based on autologous BM-MNCs transplantation in patients affected by severe limb ischemia have been recently carried out [Tateishi-Yuyama et al., 2002].

Although BM-MNCs have been proven to be effective in ischemic limbs, their collection requires general anesthesia and a large amount of marrow. Recently, Iba et al. demonstrated that nonmobilized PBMNCs can augment angiogenesis and promote ischemia recovery [Iba et al., 2002]. However, compared with BM-MNCs, implantation of nonmobilized PBMNCs did not have a good therapeutic effectiveness due to low $CD34^+$ cell concentration [Tateishi-Yuyama et al., 2002]. In contrast, different conclusion was drawn by Inaba and colleagues that implantation of nonmobilized PBMNCs was similar to that of BM-MNCs [Inaba et al., 2002]. When reported, the results differed largely among studies and the routes of cell administration, some even being controversial. Recently, we used mobilized peripheral blood mononuclear cells (M-PBMNCs) as a novel effective approach for severe diabetes foot in patients [Huang et al., 2005], but the exact mechanism of its action still remains largely undefined. Therefore, this work is to investigate the mechanism by which M-PBMNCs transplantation improves tissue ischemia.

METHODS

Cell Preparation

PBMNCs were manipulated according to standard protocols approved by the Institutional Review Board of CAMS & PUMC, and written informed consent was obtained from all healthy volunteers. M-PBMNCs were obtained from healthy donors who received treatment with rhG-CSF 600 μg/day by subcutaneous injection for 5 days. The purities of PBMNCs were >97%, as determined by differential leukocyte scattergram analysis (XE-2100, sysmex). For vessel-like tubes formation, M-PBMNCs labeled with 1, 1′-dioctadecyl-3′, 3, 3′, 3′-tetramethylindocarbocyanine labeled acetylated low-density lipoprotein (CM-DiI, Molecular Probes) were cocultured with human umbilical vein endothelial cells (HUVECs) at 1:1 cell number on matrigel and observed 24 h later.

Animals

All procedures were performed on male athymic nude mice (7–8 weeks, 16–20 g; Institute of Experimental Animal, Beijing, China) according to Peking Union Medical College Animal Care and Use Committee guidelines. Mice received streptozotocin 40 mg/kg i.p. (Sigma) in 0.05 mol/L citrate buffer, pH 4.5, daily for 5 days [Emanueli et al., 2002]. Only mice showing consistently elevated fasting glucose levels (250 mg/dl) and overt glycosuria were included in the study. If mice lost more than 20% of their body weight during the study, we discontinued their analysis. For severe ischemia model, diabetic mice were anesthetized with 50 mg/kg sodium pentobarbital i.p. and undergone femoral artery ligation. In the next day, mice were transplanted with PBS, 10^6 HUVECs, M-PBMNCs intramuscularly into the adductor muscle (four sites) with the use of a 26-gauge needle.

Detection of Apoptosis

DNA fragmentation was determined by the TUNEL assay (Roche). Deparaffinized 4 μm-thick sections were stained with FITC-conjugated antibody and then counterstained with DAPI (Sigma). Sections were examined in a blinded fashion and TUNEL-positive cell density was calculated as number of apoptotic cells per square millimeter of section.

Analysis of Limb Perfusion, Function and Ischemia Damage

Laser Doppler perfusion image (LDPI, Lisca AB, Linkoping, Sweden) was used to assess the extent of blood-flow restoration in mice after surgery. Measurements were done before surgery and at day 1, 3, 7, 14, and 28 postoperation. The images were subjected to computer-assisted quantification of blood flow, and the perfusion index was expressed as the ratio of left

(ischemic) to right (nonischemic) limb blood flow. A semiquantitative functional assessment of the ischemic limb was performed by a blinded observer using a modification of a clinical score [Kinnaird et al., 2004] (0 = toe flexion, 1 = foot flexion, 2 = no dragging but no plantar flexion, 3 = foot dragging). Ischemic damage was scored according to three different outcomes: limb salvage, necrosis, and autoamputation.

Histological Assessment of Ischemic Tissue

Deparaffinized 4 μm-thick sections of adductor muscles were stained with antimouse CD31 (BD) followed by incubation with FITC-conjugated secondary antibody. Five fields were randomly selected for capillary counts and the capillary/muscle fiber ratio was also determined. Frozen sections of 5 μm-thickness were counterstained with CD31 antibody (DAKO) or bandeiraea simplicifolia lectin 1(BS-1) lectin followed by incubation with FITC or TRITC-conjugated secondary antibodies. The capillary ECs were counted under light microscopy to determine the capillary density. To ensure that capillary densities were not overestimated as a consequence of myocyte atrophy or underestimated because of interstitial edema, the capillary/muscle fiber ratio was determined. For identification of arterioles, sections were stained with a mouse monoclonal anti-α-smooth muscle actin (α-SMactin, Sigma). Arteriole density per square millimeter of section (n art/mm^2) was then calculated. AntiVEGF polyclonal antibody (Santa Cruz), rabbit antibFGF polyclonal antibody (Santa Cruz) was used to detect the expression of angiogenic cytokine in the ischemic tissue, followed by FITC conjugated second antibody for visualization. Nonspecific immunoglobulins were used as control for the above immunohistochemistry.

Detection of Locally Delivered M-PBMNCs

Seven, 14, 28 days after Dil-labled M-PBMNCs transplantation, mice were euthanized with an overdose of pentobarbital, and ischemic tissue was obtained. Multiple frozen sections of 5 μm thick were prepared and examined under fluorescence microscopy and frozen sections of 100 μm were sequentially scanned using a confocal microscope (Leica Microsystems, GmbH). vWF, BS-1 lectin was used to detect murine ECs. Both the rhodamine and fluorescein filters were used for each image collected during the scanning process. For in vivo proliferation of implanted cells, Ki67 antibody was used (Sigma). For in situ differentiation of M-PBMNCs, mice received an intravenous injection of 100 μg FITC—Ulex europaeus agglutinin (UEA) 30 min before euthanasia.

EPC Culture and Characterization

Mononuclear cells ($10^6/mm^2$) were plated on culture dishes (BD) coated with human fibronectin (Sigma) and maintained in EC basal medium-2 supplemented with EGM-2 MV single aliquots (Clonetics, Cambrex). After 7 days in culture, adherent cells ($2–3 \times 10^5$) were immunostatined with antihuman antibodies: CD31, vWF, VE-Cadherin, KDR, CD34, CD45, CD3, CD19. Isotype matched mouse immunoglobulin served as controls. Cells were quantitatively analyzed using FACSCalibur™ and CellQuest software (BD). Attached cells were stained for the uptake of Dil-acLDL and the binding of FITC UEA (Vector Lab). Dual-positive cells were deemed EPCs and quantified by examining five random microscopic fields (×200).

Angiogenesis Assay Using the Matrigel Model

All procedures were performed on male athymic nude mice (7–8 weeks, 16–20 g; Institute of Experimental Animal, Beijing, China) according to Peking Union Medical College Animal Care and Use Committee guidelines. Mice were anesthetized with 50 mg/kg sodium pentobarbital i.p. and received in their back 0.5 ml subcutaneous injection of either Matrigel + VEGF (50 ng), Matrigel + bFGF (300 ng), Matrigel + 1×10^6 M-PBMNCs (CM-Dil-labeled), or Matrigel + 20 μl conditioned media (CM). As for CM, M-PBMNCs (1×10^7/ml) were cultured in 1,640 + 10% FBS for 4 days and CM were harvested and concentrated with Centricon Centrifugal Filter YM-3 (Amicon Bioseparations). After injection, the Matrigel formed rapidly a subcutaneous plug that was left for 21 days before removal. On day 21, the mice were euthanized and the skins were pulled back to expose the Matrigel as previously described [Iba et al., 2002]. Plugs were removed and fixed with 3.7% formaldehyde at 4°C for 12 h, embedded in paraffin, sectioned, and stained with hematoxylin and eosin (HE) or antiCD31 antibody. The tissue section was then incubated with HRP-conjugated second antibody and visualized by DAB. Matrigel plugs

were sampled systematically, obtaining three successive sections of 5 μm, at the top, middle, and bottom of each plug for microscopic examination.

Noninvasive In Vivo Imaging

Noninvasive in vivo fluorescence imaging was applied to track Dil-labled M-PBMNCs after transplantation. Mice were anesthetized with pentobarbital 40 mg/kg i.p. and placed under imaging device. Spectrally resolved images were taken from 500 to 720 nm at 10 nm intervals using a prototype of the CRI Maestro in vivo imaging system [Gao et al., 2004]. The resulting spectral data were unmixed using software provided with the system (Nuance 1.3.0). To detect the angiogenesis in matrigel, 20 min before imaging, mice received an intravenous injection of 100 μg FITC BS-1 lectin. The injected FITC BS-1 lectin will reach the matrigel and stained the vessel-supplied tissue green if vessels form in the matrigel. Dil-labeled M-PBMNCs will be shown in red.

Distribution of Cells Delivered Systemically

To investigate the distribution of circulating cells, we first labeled the cells with nuclei dye (Hoechst 33342) followed by infusion intravenously into the ischemic mice. Fourteen days later, at 30 min before the animals were euthanized, mice received an intravenous injection of 100 μg FITC BS-1 lectin. Tissues, including heart, liver, spleen, lung, and muscles of ischemic/nonischemic limbs were then obtained. Frozen sections of 5 μm thickness were examined under fluorescence microscope.

RT-PCR

RNA was extracted from 10^6 M-PBMNCs using Trizol (Invitrogen, Carlsbad, CA). Complemental DNA was synthesized using Moloney Murine Leukemia Virus Reverse Transcriptase (M-MLV RT, Invitrogen) at 37°C overnight. PCR amplification of human VEGF, bFGF, TGF-β, TNFα, IL-1β, and SDF-1 segments was performed using Taq DNA plymerase in 50 μl PCR reaction mixtures. β-actin was amplified as a reference. Their primers were as followed: VEGF (forward, 5′-CCA TGA ACT TTC TGC TGT CTT-3′; reverse, 5′-ATC GCA TCA GGG GCA CAC AG-3′); bFGF (forward, 5′-AAG AGC GAC CCT CAC ATC AA-3′; reverse, 5′-TCG TTT CAG TGC CAC ATA CC-3′); TGF-β (forward, 5′-GCT GCT GTG GCT ACT GGT GC-3′; reverse, 5′-CTT GTC ATA GAT TTC GTT GTG GG-3′); TNFα (forward, 5′-CCT GGT ATG AGC CCA TCT ATC-3′; reverse, 5′-CGA AGT GGT GGT CTT GTT GC-3′); IL-1β (forward, 5′-AGT GGC AAT GAG GAT GAC-3′; reverse, 5′-ATG AAG GGA AAG AAG GTG-3′); SDF-1 (forward, 5′- CCC TTC AGA TTG TAG CCC GG; reverse, 5′- CGA TCC CAG ATC AAT GTG CC-3′); β-actin (forward, 5′-CAG AGC AAG AGA GGC ATC C'; reverse, 5′-CTG GGG TGT TGA AGG TCT C-3′). The reverse transcription PCR-amplified samples were visualized on 1% agarose gels using ethidium bromide.

Statistics

Results are expressed as mean ± SEM. Statistical significance of differences between groups was analyzed by ANOVA followed by Fisher's *t*-test for comparison between any two groups. Statistical significance was assumed at a value of $P < 0.05$.

RESULTS

Hindlimb Blood Flow, Function, and Ischemia Damage Recovery

To analyze limb blood perfusion of severe ischemic hindlimb, LDPI analysis was performed (Fig. 1A). Diabetic mice treated with M-PBMNCs showed a significant improvement in the restoration of flow after surgery compared with PBS or HUVECs treated group (68 and 51% increase, respectively, at day 28, $P < 0.05$) (Fig. 1B). The improved flow recovery was associated with improved hindlimb appearance and function. Mice receiving PBS or HUVECs had significant impairment of ambulatory function at day 28, and was much less in the M-PBMNCs group (Fig. 1C). Similarly, mice receiving PBS or HUVECs experienced severe ischemic damage, resulting in a 40–45% incidence of auto-amputation by day 28 (Fig. 1D,E), compared to 15% in mice receiving M-PBMNCs.

Increase of Vessels With Less Apoptosis

At postoperative day 7, 14, 28, immunohistochemical analysis of CD31, BS-1 lectin in the ischemic tissues displayed a significant increase in the capillary density following transplantation of M-PBMNCs compared with the HUVECs or PBS controls (Fig. 2A,B). Apoptosis was drastically suppressed, as the number of TUNEL-positive cells in M-PBMNCs group was much less than those of the PBS group

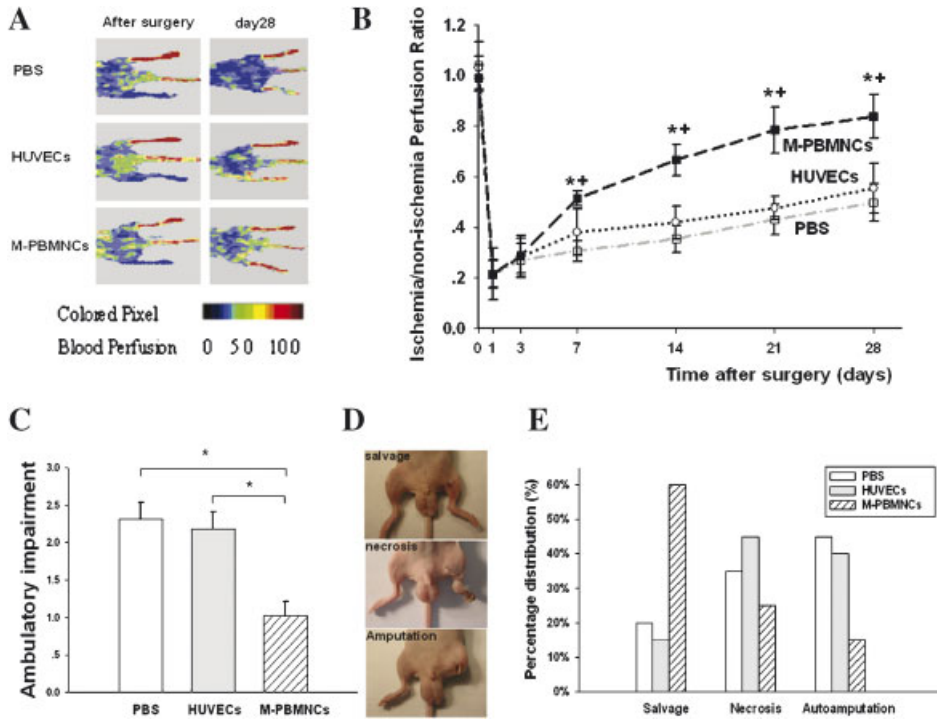

Fig. 1. Improved blood perfusion and function. **A**: Representative LDPI. In color-coded images, high blood flow is depicted in red, while low perfusion is displayed as blue to dark. **B**: Quantitative analysis of perfusion recovery measured by LDPI at each point. n = 5. $^*P < 0.05$ versus PBS, $+P < 0.05$ versus HUVECs. **C**: Effects on ambulatory impairment ($^*P < 0.05$). n = 20. **D**: Representative macroscopic photographs showing three different outcomes. From top to bottom: salvage; necrosis; amputation. **E**: Percent distribution of above outcomes among diabetic mice receiving M-PBMNC, HUVECs, or control PBS (n = 20). [Color figure can be viewed in the online issue, which is available at www.interscience.wiley.com.]

(Fig. 2C,D). The therapeutic action was also evident at the arteriole level, as the arteriole density of M-PBMNCs-treated muscles exceeded by 63.5 and 56.9% that of PBS or HUVECs-treated muscles, respectively, with the increased encompassing vessels of nearly all sizes of luminal diameter (Fig. 2E,F).

Participation of M-PBMNCs in Neovascularization

In vitro incorporation of Dil-labeled M-PBMNCs into unlabeled HUVECs networks was identified (Fig. 3A:b). In vivo fluorescence image showed implanted M-PBMNCs labeled with Dil survived at days 14 and 28 (Fig. 3A:a). A constellation of scattering transplanted cells at day 28 was seen in the frozen sections of the tissue (Fig. 3A:c). Serial scanning of tissue using confocal microscopy spatially disclosed the incorporation of implanted cells into capillary network in three dimensions (Fig. 3B). Some M-PBMNCs (red, arrows) were found to be proliferating in vivo (green) (Fig. 3C), and some differentiated in situ into endothelial lineage cells (Fig. 3D). To further verify these findings, we use vWF to stain both human and murine endothelial cells and identify some Dil^+vWF^+ cells (Fig. 3F), indicating transplanted human cells participated into vascular network in vivo.

Contribution of Angioblasts and Angiogenic Factors

The expression profile of cultured EPCs included CD31 ($84.9 \pm 8.5\%$), vWF ($63.7 \pm 9.5\%$), KDR ($61.3 \pm 14.3\%$), VE-cadherin ($74.6 \pm 12.6\%$), CD34 ($38.5 \pm 14.1\%$) and were negative for T or B lymphocyte markers (data not shown). In addition, most of the attached cells have endocytose acLDL and bound UEA (Fig. 4A). Significantly more EPCs developed from M-PBMNCs at day 7 of culture compared with the control (124 ± 10.2 vs. 75 ± 8.3 per $\times 200$ field, $P < 0.05$) (Fig. 4B), suggesting that more angioblasts were available in M-PBMNCs. By RT-PCR, we detected that M-PBMNCs contained a group of angiogenic factors and cytokines, including VEGF, bFGF, TGF-β, TNF-α, IL-1β, and SDF-1 (Fig. 4C RT-PCR). Western blotting

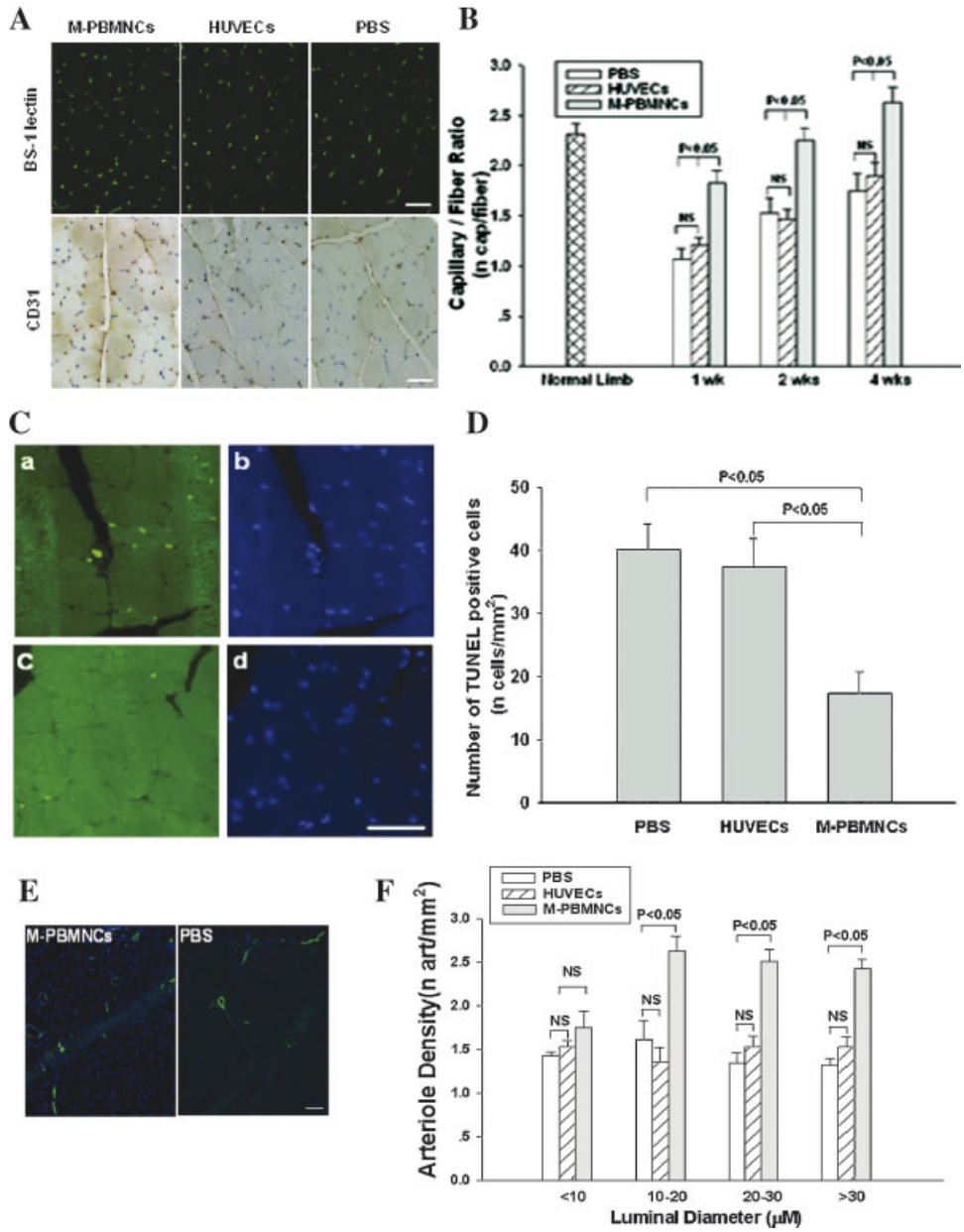

Fig. 2. Increased capillary density and decreased apoptosis. **A**: Endothelial cells were stained with BS-1 lectin, CD31. **B**: By CD31, capillary/fiber ratio significantly increased in mice receiving M-PBMNCs versus HUVECs or PBS. **C**,**D**: Positive nuclei for DNA fragmentation (**a**,**c**) were revealed in green, and sections were counterstained with DAPI (**b**,**d**). Less apoptosis was detected in sections of M-PBMNCs-treated muscles (c,d) than PBS group (a, b). Bar = 50μm, n = 5. **E**: Representative figures of arterioles (green) in M-PBMNCs treated or PBS injected tissue. **F**: Arteriole density of different sizes significantly increased in diabetic mice receiving M-PBMNCs versus HUVECs or PBS at 4 week postoperatively (n = 5 for each group). [Color figure can be viewed in the online issue, which is available at www.interscience.wiley.com.]

revealed significantly higher local adductor muscle production of bFGF and VEGF in those mice receiving M-PBMNCs and BM-MNCs compared with mice receiving PBS (Fig. 4C Western). To confirm that M-PBMNCs secreted arteriogenic cytokines in vivo, sections were examined for colocalization of M-PBMNCs and VEGF and bFGF (arrows indicate $VEGF^{+}Dil^{+}$ or $bFGF^{+}Dil^{+}$ cells, Fig. 4D). Serial scans of vessels using confocal microscopy spatially disclosed in three dimensions the distribution of pericytes/SMCs (red) marked by α-SMactin around the endothelial cells (green, Fig. 4E). Nuclei were shown in blue (Fig. 4F). So the pericytes/SMC and ECs were demonstrated by using different antibodies, which did not

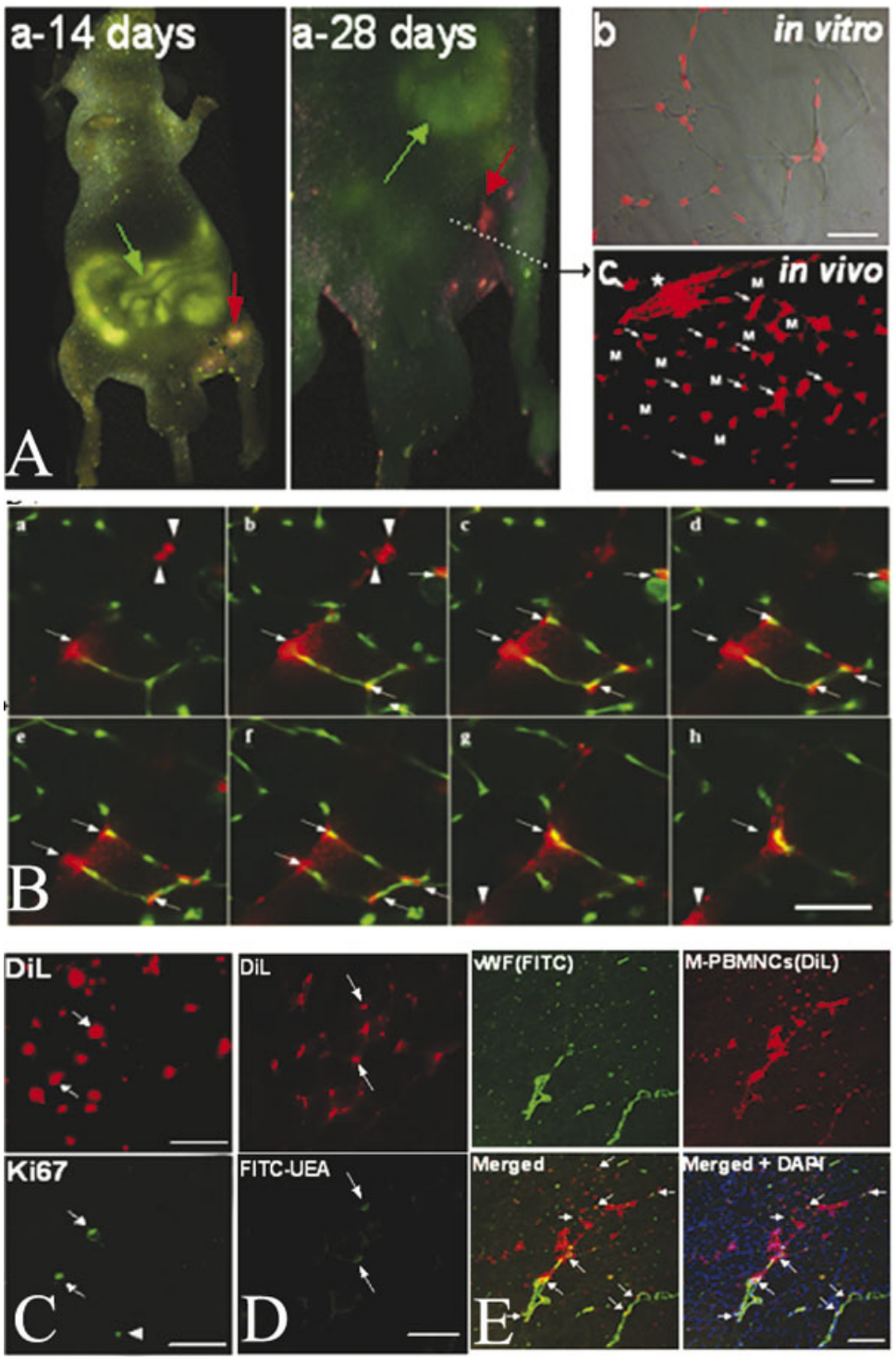

Fig. 3. Survival, migration, proliferation, differentiation, and vessel incorporation of M-PBMNCs in vivo. **A**: Angiogenesis like network was observed 24 h after coculture of HUVECs and DiI-labeled M-PBMNCs on matrigel (**b**). In vivo fluorescence image of mice (**a**) shows transplanted M-PBMNCs (red arrows) and food fluorescence (green arrows). Implanted M-PBMNCs (**c**) were sprouting from a place near the cell injection site indicated by *, and they (arrows) further migrated into the interstitial regions among preserved skeletal myocytes (M). **B**: A series of 40 focal plans was acquired 3 μm apart (**a**–**h**). Notice the DiI-labeled M-PBMNCs (arrows) incorporated into the vasculature delineated by the green fluorescence (BS lectin-1), while some had not incorporated into vasculature (arrowheads). **C**: Arrows indicate $Ki67^{+}DiI^{+}$ cells, while arrowhead suggests murine proliferating cells. **D**: Human EC specific marker UEA identifies transplanted M-PBMNCs (DiI) as endothelial lineage cells (green, arrows). **E**: M-PBMNCs (red, arrows) participated in vessel network indicated by vWF (green). [Color figure can be viewed in the online issue, which is available at www.interscience.wiley.com.]

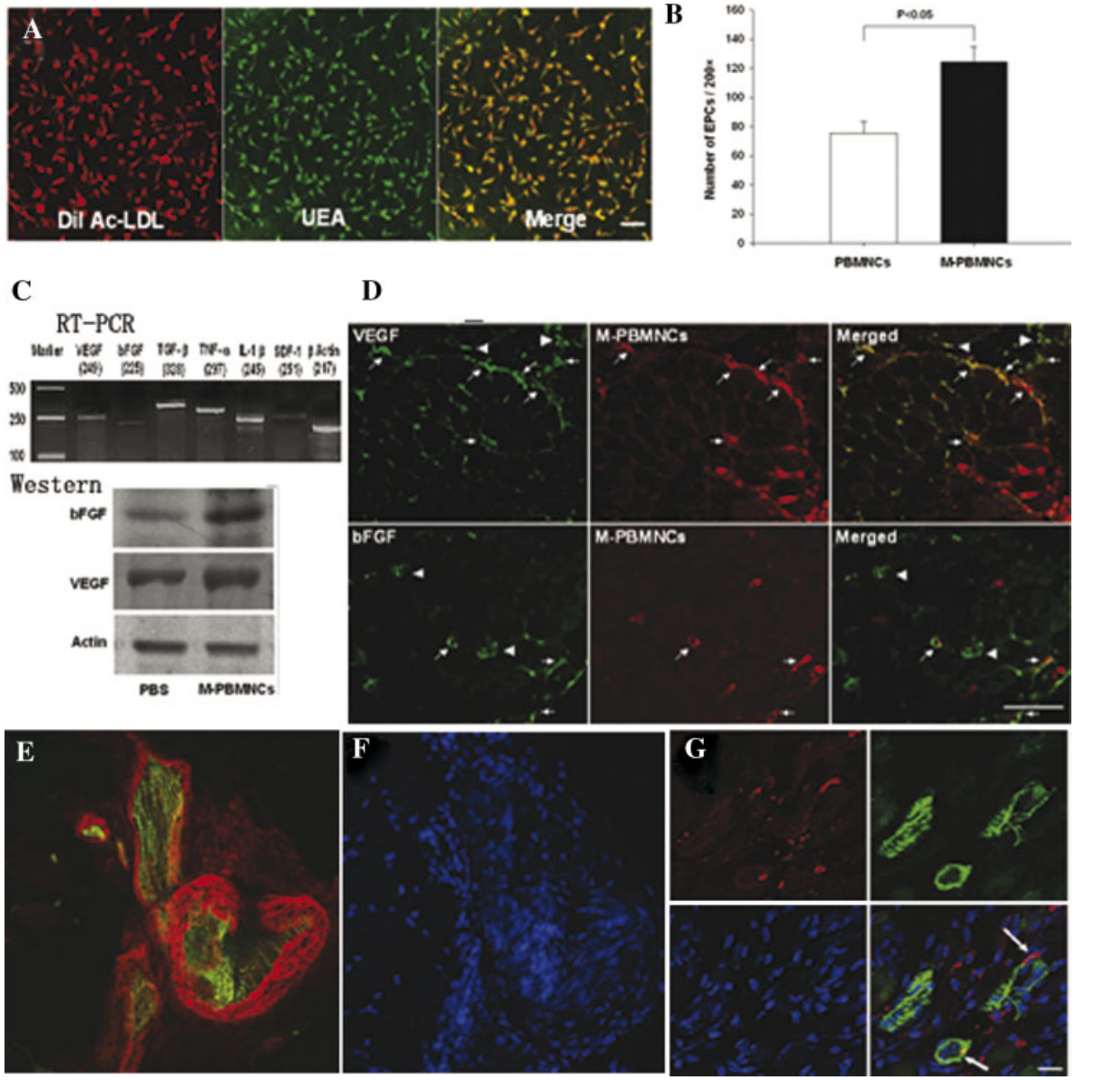

Fig. 4. Supply of abundant angioblasts and angiogenic factors. **A**: The attached cells of M-PBMNCs and BM-PBMNCs took up Dil-AcLDL (red) and bound FITC-UEA (green). **B**: Quantification of attached cells showed that more EPCs could be cultured from blood cells after mobilization. **C**: RT-PCR showed M-PBMNCs contained many kinds of angiogenic factors and cytokines, including VEGF, bFGF, TGF-β, TNF-α, IL-1β, TNF-1. Western blotting (day 7) demonstrating that injection of M-PBMNCs increased local production of VEGF and bFGF compared with PBS injection. Actin was used as control. **D**: Expression of VEGF, bFGF in vessel walls (green) corresponded to red M-PBMNCs (arrows), and paracrine secretion of VEGF/bFGF in murine cells could be noted (arrowheads). **E**,**F**: 3-D figure of vessel that are covered with pericytes/SMCs (red) outside the ECs (green). Nuclei are stained in blue (right panel). **G**: Some Dil-labeled M-PBMNCs (red, arrows) showed α-SMactin positive (green). Nuceli are stained in blue. Bar = 50 μm. [Color figure can be viewed in the online issue, which is available at www.interscience.wiley.com.]

cross-react with each other. Dil^{+}-labeled M-PBMNCs (red) were found to incorporate into vessel and were α-SMactin positive (green, Fig. 4G), indicating some M-PBMNCs acquired smooth muscle cell marker and may contribute to the maturation of forming vessels.

Proangiogenesis Ability of M-PBMNCs and its CM

We used the matrigel plug as angiogenesis induction method to study the in vivo role of VEGF, bFGF, M-PBMNCs, and CM. When the

Matrigel plugs were implanted subcutaneously into the flank of mice, angiogenesis was induced with the various stimulators in the Matrigel. We applied fluorescence imaging as a novel method for detection of vessel formation in the matrigel. Figure 5A shows the process of unmixed pseudocolor images from original RGB images by using CRI Maestro in vivo imaging system. In the pseudocolor images, matrigel+Dil-cells were shown red fluorescence while matrigel without Dil-cells (control) exhibited no red fluorescence. Mice injected with FITC-BS lectin-1 were shown in green fluorescence except for the matrigel-injected area. For the control mice, no green fluorescence was detected. At day 21, M-PBMNCs containing-matrigel plug (red) was infiltered by green fluorescence (BS-1 lectin). Since systematically injected BS lectin (green) could only reach tissue that was supplied with blood vessels, green fluorescence in the matrigel plug suggest that vessels had penetrated the matrigel (Fig. 5B). At day 21, most area of M-PBMNCs containing-matrigel was covered in green, while the control still exhibited area without vessel supply. These data suggest that M-PBMNCs, when transplanted in vivo, can promote vessel growth. Figure 5C shows the macroscpic view, HE and CD31 staining of matrigel plugs. Arrows indicated vessels with erythrocytes inside. More vessels were observed in the groups impregnated with VEGF, bFGF, M-PBMNCs, or CM than in the control (Fig. 5C).

Local Delivery Versus Systemic Delivery

We delivered M-PBMNCs to mice systemically by intravenous injection as well as locally by intramuscular injection. To detect the transplanted cells, sections of different tissues were compared under fluorescence microscopy. A great many Hoechst-stained circulating mononuclear cells (blue) delivered intravenously into mice were detained in the liver and spleen, but seldom seen in the heart or nonischemic limb (upper panel, Fig. 6). When Dil-labeled M-PBMNCs were delivered locally to the ischemic hindlimbs, few cells could be detected in tissues outside the ischemic limb (lower panel, Fig. 6).

DISCUSSION

Therapeutical implantation of M-PBMNCs into severe ischemic hind limb resulted in the promotion of limb perfusion and function as well as amelioration of ischemia damage. The transplantation of M-PBMNCs for ischemic limbs in diabetes was effective, suggesting it was a promising alternative approach for diabetic complications. We demonstrated the survival, migration, proliferation, differentiation of M-PBMCs into EC-lineage and α-SMactin$^+$ cells in situ, and their incorporation into murine capillary vessel walls. In addition, they also supplied angiogenic cytokines (e.g. VEGF, bFGF) that promoted vessel growth in ischemic hindlimbs. Augmented vessel formation in matrigel plug confirmed the proangiogenic ability of M-PBMNCs.

In our experiments, we chose diabetic mice model instead of normal one to mimic the clinical settings. Diabetes impaired the therapeutic efficacy of bone marrow cells transplantation for limb ischemia [Tamarat et al., 2004]. This was due to microagniopathy induced by diabetes [Emanueli et al., 2002] and reduced number as well as dysfunction of EPCs from STZ-mice (data not shown). EPCs have an important role in repairing injured vessels by migrating to ischemia sites and forming new vasculature de novo (vasculogenesis) [Asahara et al., 1997; Asahara et al., 1999a]. The therapeutic efficacy of these dysfunctional EPCs from STZ-mice was compromised. In addition, less number of both capillaries and arterioles could be detected during the time course of diabetes [Currie et al., 1998]. As a result, the efficacy of M-PBMNCs in STZ-mice differ from that in normal (no STZ treatment) nude mice. In this sense, selection of different animal models may greatly influence the final data, thus we chose STZ-mice, instead of normal mice.

Therapeutic neovascularization is an important strategy to salvage tissue from critical ischemia and the cell-based therapeutic strategy in augmenting neovascularization is now a new research focus. BM-MNCs have been shown to enhance angiogenesis in animal and human ischemic hindlimbs or infracted myocardium [Ikenaga et al., 2001; Kocher et al., 2001; Shintani et al., 2001]. However, BM could not always be available due to various reasons such as chemotherapy, radiotherapy, or heavy tumor infiltration. It is also difficult to collect sufficient quantity of bone marrow for such transplantation. M-PBMNCs have several advantages [Pecora et al., 2002]. After mobilization, they may contain far more CD34$^+$ cells

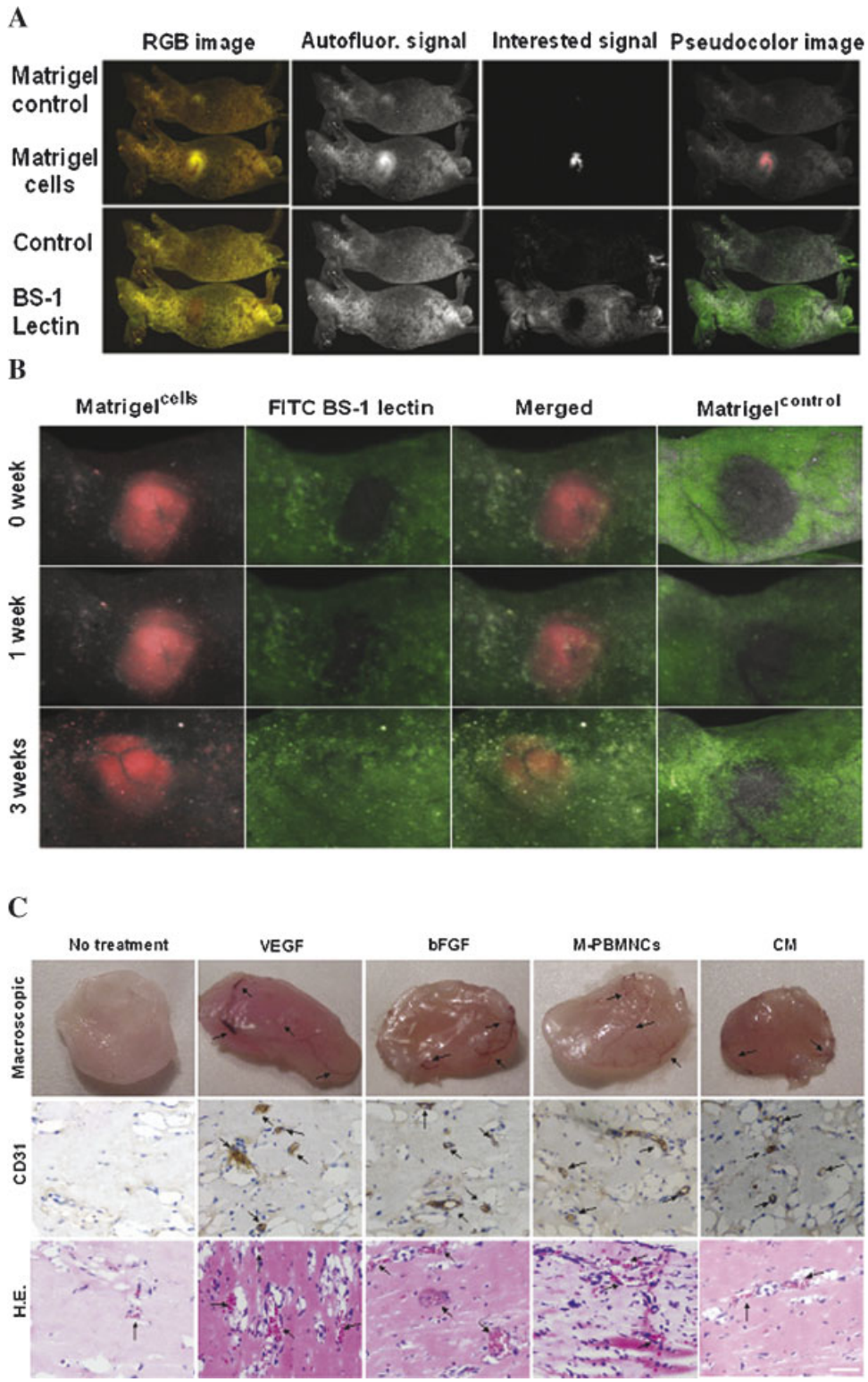

Fig. 5. Angiogenesis in matrigel plug. **A**: RGB images were obtained, computed, unmixed and added with pseudocolors. Mice transplanted in the right flank with matrigel were used as a control (matrigel^{control}) for mice transplanted with matrigel + DiI-labeled M-PBMNCs (matrigel^{cells}). Mice injected intravenously with PBS were selected as control for mice injected with BS-1 lectin (FITC). **B**: Representative images of mice transplanted with matrigel^{control} or matrigel^{cells}. At day 1, red fluorescence was detected in matrigel^{cells}, and the green fluorescence surrounded its margin. Neither red nor green fluorescence was observed in matrigel^{control} area. At day 21, infiltration of green fluorescence could be detected in matrigel^{cells}, and merge of red and green fluorescence were shown as yellow. **C**: Macroscopic view, HE and CD31 staining revealed vessels (arrows) in VEGF, bFGF groups, but seldom in the control group. M-PBMNCs and CM also stimulated vessel growth compared with the control. Bar = 50 μm. [Color figure can be viewed in the online issue, which is available at www.interscience.wiley.com.]

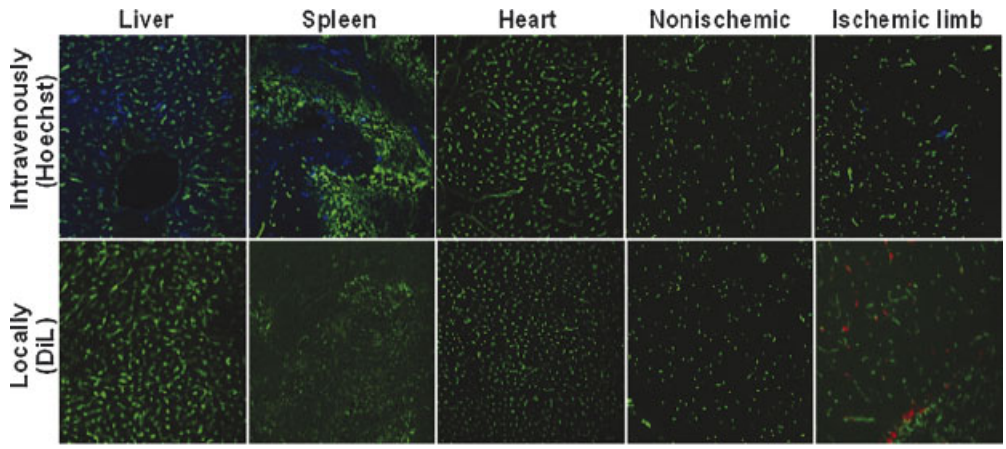

Fig. 6. Systemic versus local transplantation. Mice vessels were stained with FITC-BS lectin-1 (green). Intramuscularly delivered M-PBMNCs were labeled with Dil (red), while intravenously delivered M-PBMNCs were stained with Hoechst 33342 (blue). A great many circulating mononuclear cells (blue) were detained in the liver and spleen, but seldom seen in heart or nonischemic limb (**upper panel**). When Dil-labeled M-PBMNCs were delivered locally into ischemic hindlimbs, few cells could be detected in tissues outside the ischemic limb (**lower panel**). [Color figure can be viewed in the online issue, which is available at www.interscience.wiley.com.]

than steady-state BM [Korbling and Anderlini, 2001]. The various mobilization regimens lead to a concentration of $CD34^+$ cells in the peripheral blood that is similar to, or even higher than that in steady-state bone marrow [Jansen et al., 2005]. Murohara and colleagues discovered that when $CD34^+$ and $CD34^-$ cells were separately cultivated and the number of EPCs was counted 7 days later, more EPCs developed from $CD34^+$ group [Schatteman et al., 2000]. Their result supports our findings that more EPCs could be cultured from mobilized blood cells since they contained more $CD34^+$ cells. Our results showed that $CD34^+$ cell abundant M-PBMNCs augmented the ischemia-induced neovascularization, which was in accordance with the previous data that $CD34^+$ cells accelerate the rate of blood-flow restoration in mice undergoing neovascularization due to hindlimb ischemia [Schatteman et al., 2000].

The improved limb perfusion with salvage of the severely ischemic limb was related to reduced apoptosis and increased capillary proliferation. Injection of M-PBMNCs attenuated the EC apoptosis, as they migrated into interstitial regions of skeletal muscles, attached to and incorporated with the murine ECs. Such physical cell-to-cell contact may be crucial for the survival of apoptotic ECs, and can augment neovascularization by provoking murine ECs proliferating [Murohara et al., 2000]. In addition, M-PBMNCs were found to attach to the vessel wall and some differentiated into smooth muscle cells, which promoted the maturation and stabilization of newly forming blood vessels.

Poor blood vessel growth in ischemic limbs and increased angiogenesis in retinal complications is a "diabetic paradox" [Fadini and Avogaro, 2006]. This is attributed to the differential regulation of angiogenic factors in the retina versus the systemic circulation. Although systemic increase of mononuclear cells has been reported to benefit hindlimb ischemia, we intentionally choose local M-PBMNCs for the present study to avoid abnormal vasculogenesis in other tissues, especially the retina. The absence of obvious transplanted cells in organs outside the injected hindlimb (Fig. 6) suggested the safety of this approach. Moreover, local transplantation of M-PBMNCs directly brought the angioblasts into the pathological foci where progenitor cells could begin a reparative role. M-PBMNCs can also secrete a cocktail of cytokines that promote angiogenesis. Elevated VEGF expression in adductor muscles was a result of M-PBMNCs transplantation, but not a result of severe ischemia, since HIF-1α was not significantly elevated in the adductor muscels (Data not shown). In situ secretion of VEGF and bFGF by M-PBMNCs triggered the proliferation of ECs and the paracrine secretion of VEGF and bFGF by murine cells might be partly related to the angiogenic surroundings

(Fig. 4D). Thus, these cells may alter the local VEGF levels by producing the factor themselves as well as by secreting MMPs that release extracellular matrix-bound VEGF [Bergers et al., 2000]. What is more, since VEGF could contribute to postnatal neovascularization by mobilizing bone marrow-derived EPCs [Asahara et al., 1999b], VEGF secreted by M-PBMNCs may also induce mobilization of stem cells in vivo.

$CD34^+$ cells were believed to be a rich source of EPCs [Murohara et al., 2000], and mobilization increased the number of $CD34^+$ cells in M-PBMNCs. Despite the important role of $CD34^+$ cells, some $CD34^-$ cells can also take part in the capillary network, and their cell-to-cell interactions with $CD34^+$ cells may influence the roles of $CD34^+$ cells in vivo. While EPCs can also be derived from $CD34^-$ cells or $CD14^+$ monocytes [Harraz et al., 2001], the ability of monocytes/macrophages in differentiating into EPCs should also be considered. Monocytes appear to be central to arterial remodeling in tissues undergoing arteriogenesis, accumulating at sites of collateral artery growth and angiogenesis [Arras et al., 1998]. Because M-PBMNCs contain abundant monocytes, it remains to be determined whether the improvement was in part aided by the monocytic cell fraction. As a simple, safe, effective, and novel therapeutic approach for diabetic complications [Huang et al., 2005], the full potential of M-PBMNCs transplant merits further investigation.

ACKNOWLEDGMENTS

We sincerely thank Ping Ping Huang, Shang Zhu Li, Yu Ling Zhou, Hui Shu Chen for great help in cell collection and technical guidance. We also express our heartfelt gratitude towards Ya Zhong Ke, Fei Wu, Ning Li, Yan Cao from Ming-Mei Technology Co. for technical help in the processing of in vivo images.

REFERENCES

Arras M, Ito WD, Scholz D, Winkler B, Schaper J, Schaper W. 1998. Monocyte activation in angiogenesis and collateral growth in the rabbit hindlimb. J Clin Invest 101:40–50.

Asahara T, Masuda H, Takahashi T, Kalka C, Pastore C, Silver M, Kearne M, Magner M, Isner JM. 1999a. Bone marrow origin of endothelial progenitor cells responsible for postnatal vasculogenesis in physiological and pathological neovascularization. Circ Res 85:221–228.

Asahara T, Murohara T, Sullivan A, Silver M, van der Zee R, Li T, Witzenbichler B, Schatteman G, Isner JM. 1997. Isolation of putative progenitor endothelial cells for angiogenesis. Science 275:964–967.

Asahara T, Takahashi T, Masuda H, Kalka C, Chen D, Iwaguro H, Inai Y, Silver M, Isner JM. 1999b. VEGF contributes to postnatal neovascularization by mobilizing bone marrow-derived endothelial progenitor cells. Embo J 18:3964–3972.

Bergers G, Brekken R, McMahon G, Vu TH, Itoh T, Tamaki K, Tanzawa K, Thorpe P, Itohara S, Werb Z, Hanahan D. 2000. Matrix metalloproteinase-9 triggers the angiogenic switch during carcinogenesis. Nat Cell Biol 2:737–744.

Currie CJ, Morgan CL, Peters JR. 1998. The epidemiology and cost of inpatient care for peripheral vascular disease, infection, neuropathy, and ulceration in diabetes. Diabetes Care 21:42–48.

Eckardt A, Kraus O, Kustner E, Neufang A, Schmiedt W, Meurer A, Schollner C, Schadmand-Fischer S. 2003. Interdisciplinary treatment of diabetic foot syndrome. Orthopade 32:190–198.

Emanueli C, Salis MB, Pinna A, Stacca T, Milia AF, Spano A, Chao J, Chao L, Sciola L, Madeddu P. 2002. Prevention of diabetes-induced microangiopathy by human tissue kallikrein gene transfer. Circulation 106: 993–999.

Fadini GP, Avogaro A. 2006. Autologous transplantation of granulocyte colony-stimulating factor-mobilized peripheral blood mononuclear cells improves critical limb ischemia in diabetes. Diabetes Care 29:478–479; author reply 479–480.

Folkman J. 1998. Therapeutic angiogenesis in ischemic limbs. Circulation 97:1108–1110.

Gao X, Cui Y, Levenson RM, Chung LW, Nie S. 2004. In vivo cancer targeting and imaging with semiconductor quantum dots. Nat Biotechnol 22:969–976.

Harraz M, Jiao C, Hanlon HD, Hartley RS, Schatteman GC. 2001. CD34—blood-derived human endothelial cell progenitors. Stem Cells 19:304–312.

Hasson E, Arbel D, Verstandig A, Shimoni Y, Mitrani E. 2005. A cell-based multifactorial approach to angiogenesis. J Vasc Res 42:29–37.

Huang P, Li S, Han M, Xiao Z, Yang R, Han ZC. 2005. Autologous transplantation of granulocyte colony-stimulating factor-mobilized peripheral blood mononuclear cells improves critical limb ischemia in diabetes. Diabetes Care 28:2155–2160.

Iba O, Matsubara H, Nozawa Y, Fujiyama S, Amano K, Mori Y, Kojima H, Iwasaka T. 2002. Angiogenesis by implantation of peripheral blood mononuclear cells and platelets into ischemic limbs. Circulation 106:2019–2025.

Ikenaga S, Hamano K, Nishida M, Kobayashi T, Li TS, Kobayashi S, Matsuzaki M, Zempo N, Esato K. 2001. Autologous bone marrow implantation induced angiogenesis and improved deteriorated exercise capacity in a rat ischemic hindlimb model. J Surg Res 96:277–283.

Inaba S, Egashira K, Komori K. 2002. Peripheral-blood or bone-marrow mononuclear cells for therapeutic angiogenesis? Lancet 360:2083; author reply 2084.

Ingram DA, Mead LE, Tanaka H, Meade V, Fenoglio A, Mortell K, Pollok K, Ferkowicz MJ, Gilley D, Yoder MC.

2004. Identification of a novel hierarchy of endothelial progenitor cells using human peripheral and umbilical cord blood. Blood 104:2752–2760.

Jansen J, Hanks S, Thompson JM, Dugan MJ, Akard LP. 2005. Transplantation of hematopoietic stem cells from the peripheral blood. J Cell Mol Med 9:37–50.

Kinnaird T, Stabile E, Burnett MS, Shou M, Lee CW, Barr S, Fuchs S, Epstein SE. 2004. Local delivery of marrow-derived stromal cells augments collateral perfusion through paracrine mechanisms. Circulation 109: 1543–1549.

Kocher AA, Schuster MD, Szabolcs MJ, Takuma S, Burkhoff D, Wang J, Homma S, Edwards NM, Itescu S. 2001. Neovascularization of ischemic myocardium by human bone-marrow-derived angioblasts prevents cardiomyocyte apoptosis, reduces remodeling and improves cardiac function. Nat Med 7:430–436.

Korbling M, Anderlini P. 2001. Peripheral blood stem cell versus bone marrow allotransplantation: Does the source of hematopoietic stem cells matter? Blood 98:2900–2908.

Murohara T, Ikeda H, Duan J, Shintani S, Sasaki K, Eguchi H, Onitsuka I, Matsui K, Imaizumi T. 2000. Transplanted cord blood-derived endothelial precursor cells augment postnatal neovascularization. J Clin Invest 105:1527–1536.

Pecora AL, Lazarus HM, Jennis AA, Preti RA, Goldberg SL, Rowley SD, Cantwell S, Cooper BW, Copelan EA, Herzig RH, Meagher R, Kennedy MJ, Akard LR, Jansen J, Ross A, Prilutskaya M, Glassco J, Kahn D, Moss TJ. 2002. Breast cancer cell contamination of blood stem cell products in patients with metastatic breast cancer: Predictors and clinical relevance. Biol Blood Marrow Transplant 8:536–543.

Rajagopalan S, Shah M, Luciano A, Crystal R, Nabel EG. 2001. Adenovirus-mediated gene transfer of VEGF(121) improves lower-extremity endothelial function and flow reserve. Circulation 104:753–755.

Schatteman GC, Hanlon HD, Jiao C, Dodds SG, Christy BA. 2000. Blood-derived angioblasts accelerate blood-flow restoration in diabetic mice. J Clin Invest 106:571–578.

Shintani S, Murohara T, Ikeda H, Ueno T, Sasaki K, Duan J, Imaizumi T. 2001. Augmentation of postnatal neovascularization with autologous bone marrow transplantation. Circulation 103:897–903.

Simons M, Annex BH, Laham RJ, Kleiman N, Henry T, Dauerman H, Udelson JE, Gervino EV, Pike M, Whitehouse MJ, Moon T, Chronos NA. 2002. Pharmacological treatment of coronary artery disease with recombinant fibroblast growth factor-2: Double-blind, randomized, controlled clinical trial. Circulation 105: 788–793.

Takahashi T, Kalka C, Masuda H, Chen D, Silver M, Kearney M, Magner M, Isner JM, Asahara T. 1999. Ischemia- and cytokine-induced mobilization of bone marrow-derived endothelial progenitor cells for neovascularization. Nat Med 5:434–438.

Tamarat R, Silvestre JS, Le Ricousse-Roussanne S, Barateau V, Lecomte-Raclet L, Clergue M, Duriez M, Tobelem G, Levy BI. 2004. Impairment in ischemia-induced neovascularization in diabetes: Bone marrow mononuclear cell dysfunction and therapeutic potential of placenta growth factor treatment. Am J Pathol 164: 457–466.

Tateishi-Yuyama E, Matsubara H, Murohara T, Ikeda U, Shintani S, Masaki H, Amano K, Kishimoto Y, Yoshimoto K, Akashi H, Shimada hK,Iwasaka T, Imaizumi T. 2002. Therapeutic angiogenesis for patients with limb ischaemia by autologous transplantation of bone-marrow cells: A pilot study and a randomised controlled trial. Lancet 360:427–435.